Efficient interfacial upconversion enabling bright emission with extremely low driving voltage in organic light-emitting diodes

Seiichiro Izawa[1,2], Masahiro Morimoto[3*], Shigeki Naka[3], and Masahiro Hiramoto[1,2]*

[1]Institute for Molecular Science, 5-1 Higashiyama, Myodaiji, Okazaki 444-8787, Aichi, Japan, [2]The Graduate University for Advanced Studies (SOKENDAI), 5-1 Higashiyama, Myodaiji, Okazaki, Aichi 444-8787, Japan. [3]Academic Assembly Faculty of Engineering, University of Toyama, 3190 Gofuku, Toyama 930-8555, Japan.

E-mail: izawa@ims.ac.jp

Abstract

Reducing operating voltage is the remaining frontier for organic light-emitting diodes (OLEDs) because their quantum efficiency (QE) of electroluminescence has been already maximized. Herein, we report an efficient OLED in which a blight emission equivalent to a luminance of a display is achieved by only a 1.5 V battery. The OLED is based on upconversion (UC) emission utilizing triplet-triplet annihilation occurring near donor/acceptor (D/A) interface. We found that a character of a charge transfer state that is key intermediate for the UC emission could be controlled by D/A interfacial interaction. As a result, parasitic loss processes for UC were greatly suppressed from over 90% to about 10%, and two order of magnitude higher QE than the previous UC-OLED was achieved. Our result demonstrated that the efficient UC could be realized by the management of the energy transfer steps at the D/A interface and utilizing UC emission can be one of the possible candidate for efficient OLED with extremely low driving voltage.

Main text

From current to photon conversion efficiency of organic light-emitting diodes (OLEDs) has been already maximized. External quantum efficiency (EQE) has exceeded 20% with internal quantum efficiency (IQE) of 100%, owing to the development of phosphorescent and thermally activated delayed fluorescence materials realizing successful spin management of excited sates.[1-2] However, operating voltage of the common types of OLED is very high due to following three reasons. Full bandgap voltage is required to form either singlet or triplet exciton of the emitter material.[3] The emitter material is generally dispersed in an amorphous host material in order to prevent aggregation quenching, however the charge mobility of the host material is generally as low as 10^{-3}~10^{-5} cm^2/Vs because of its amorphous structure,[4] decreasing a conductivity of the layer. Furthermore, multilayered structures for charge carrier injection, transport, and blocking increases the total thickness of the device, leading to a reduction of an internal electric field.[5] According to these reasons, the operating voltage of OLED emitting about 600 nm light at 100 cd/m^2, which is a general display driving condition, is very high as 4.5 V.[6]

One of the possible strategies to reduce the operating voltage of OLED is utilizing upconversion (UC) emission based on triplet-triplet annihilation (TTA) sensitized by a charge transfer (CT) state at the donor/acceptor (D/A) interface.[7-12] The active layer of UC-OLED consists of two: emitter (donor) layer playing hole transport and emission, and acceptor layer for electron transport. The operating mechanism involved in UC-OLED are as illustrated in **Figure 1a**: at first, injected charge formed both singlet and triplet CT state, denoted as CT_1 and CT_3, at the D/A interface. Subsequently, energy of the CT_3 is transferred to triplet exciton in the emitter molecule, and two triplets on the neighboring emitters, form one singlet with a higher energy, through TTA. Finally, the UC emission occurs from the emitter molecule. There are several advantages in this mechanism over the normal OLED devices: first, TTA upgrade the energy of excited state as almost twice, thus electroluminescence (EL) starts from about half voltage of the bandgap energy of emitter material.[12] Second, all the excited states for photo-emission forms near D/A interface, thus the transporting layer can be crystalline material with high

mobility, leading to the high conductivity of the layer. Third, energy gap at the D/A heterojunction interface prevent leak current, thus additional blocking layers are not required. As these reasons, the EL emission starts from less than 1 V in in rubrene/C_{60}, which is the most commonly studied combination of donor and acceptor in UC-OLED.[12] However, the critical issues to be overcome in the UC-OLEDs are their low EQE value of 0.043% in the rubrene/C_{60} combination.[9] The reason for low EQE is the existence of severe parasitic loss processes including back charge separation (BCS) from the singlet exciton of the emitter to CT_1 occurring at the D/A interface, and singlet fission (SF) that is the inverse process of TTA[11] as illustrated in **Figure 1b**. As a result, most of the excited states deactivate via ether non-radiative or radiative recombination from the CT states and the triplet exciton of rubrene that follows BCS and SF. The strategies to prevent these parasitic loss processes in the UC-OLED is desired.

In this work, efficient UC-OLED with two order of magnitude higher EQE than the previous report is realized by preventing the parasitic loss processes. The advancement is mainly based on the two strategies. Firstly, we replaced the acceptor material from C_{60} that is most commonly utilized in UC-OLED to *N*,*N'*-di-*n*-octyl-3,4,9,10-perylenetetracarboxylic diimide (C_8-PTCDI) (**Figure 1c**) that has highly crystalline edge-on structure in the thin film.[13] C_8-PTCDI has highest crystallinity among the perylene diimide derivatives with different alkyl side chain length.[14] The alkyl side chain of C_8-PTCDI standing up in the direction to the donor layer can prevent BCS by reducing the D/A interaction. Secondly, an emissive dopant was introduced into the emitter layer in order to accelerate fluorescence by resonance energy transfer (FRET) and kinetically prevent the loss processes. As the results, parasitic loss was reduced from 94% to 14%, and OLED operation of 608 nm (2.04 eV) emission with 177 cd/m^2 only by a 1.5 V battery, which is world lowest operating voltage so far, became possible.

In our experiment, we used rubrene as the TTA emitter. Rubrene satisfies the energetic requirement for efficient TTA: the energy of first excited triplet state (T_1) is 1.14 eV that is slightly larger than half of the first excited singlet state (S_1) of 2.21 eV.[15] The UC-OLED devices were fabricated by a thermal evaporation with the following planer heterojunction structure: indium tin oxide (ITO)/MoO_3 (10 nm)/Rubrene (60 nm)/Acceptor (50 nm)/LiF (0.2 nm)/MoO_3 (0.3 nm)/Al (70 nm). The control device

with 50 nm of bathocuproine (BCP) layer instead of C_{60} and C_8-PTCDI acceptor layers is also fabricated as a reference. The emissive dopant—tetraphenyldibenzoperiflanthene (DBP)—was introduced into the rubrene layer via the codeposition technique.[16] DBP was chosen because its S_1 was 2.04 eV that was slightly smaller than that of rubrene, leading to efficient FRET with small energy loss. The doping concentration of DBP was set to 0.5% because the condition exhibited the highest photoluminescence (PL) QE in the thin films among 0-5% doping concentration as summarized in **Figure S1** and **Table S1**. The thickness of DBP doped rubrene layer was 50 nm except the EQE experiment in **Figure 3** and the pristine rubrene layer (10 nm) was inserted between DBP doped rubrene and MoO_3 layers except the luminance measurement in **Figure 2a** and **b**. The energy levels of the materials are summarized in **Figure 1d**. The energy difference of highest occupied molecular orbitals (HOMOs) and lowest unoccupied molecular orbitals (LUMOs) between donor and acceptor materials are large enough to prevent leak current without additional electron and hole blocking layer and form CT state at the D/A interface.

Figure 2a and **b** present current density (*J*)-voltage (*V*) and luminance (*L*)-*V* characteristics of the UC-OLEDs and rubrene/BCP control devices. Turn-on voltage of EL emission largely shifted from 3.4 V in the rubrene/BCP control device to about 1 V in rubrene/C_{60} and rubrene/C_8-PTCDI devices. The turn-on of UC-OLEDs were smaller than the half of the band gap energy of rubrene: 2.2 eV, indicating the emitted photons were generated through TTA. Comparing the UC-OLEDs with C_{60} and C_8-PTCDI as the acceptor layer, luminance increased as large as 1.4-5.0 times at above 1.2 V from C_{60} to C_8-PTCDI. This indicates that the use of C_8-PTCDI could prevent the loss processes in the UC-OLEDs. The luminance of the UC-OLED could be further increased by DBP doping. The emission peak shifted from 565 nm in the undoped device to 608 nm in the DBP-doped device owing to the FRET from the rubrene to the DBP, and the intensity increased as 7.5 times under same injected current condition as presented in **Figure 2c**. Especially, enhancement of the luminance by DBP doping is significant at smaller applied voltage condition. Although the *J*-*V* characteristics are almost identical as shown in **Figure 2a**, the turn on voltage measured by a photodetector that is more sensitive to the weak emission than luminance meter shifted from 0.94 V in the undoped device to 0.87 V in the doped

device (**Figure 2d**). The improvement of luminance by the DBP doping is 37, 25, and 19 times at 1.0, 1.3, and 1.5 V, respectively. The result indicates that the DBP can accelerated the emission especially in smaller carrier concentration condition where TTA is generally inefficient.[17] As these results, the DBP-doped rubrene/C_8-PTCDI device reached 100 cd/m^2 at 1.33 V in the DBP emission at 608 nm (2.04 eV). To the best of our knowledge, this is the smallest operating voltage for realizing EL emission with 100 cd/m^2 in all kinds of OLEDs.[3, 11-12, 18-19] This enables the demonstration that the UC-OLED with 177 cd/m^2 can be operated only by a 1.5 V battery as presented in **Figure 2e**. Further improvement under high carrier concentration condition above 2.1 V could be realized by inserting pristine rubrene interlayer between MoO_3 and DBP doped rubrene layers. This prevents quenching of S_1 exciton in the DBP doped rubrene layer at the MoO_3 interface, resulting the luminance was improved as 1.9 times as maximum at 4.1 V. The pristine rubrene interlayer between the MoO_3 and DBP-doped rubrene layer was always inserted in the following experiments.

EQEs of the UC-OLED, as presented in **Figure 3a** and **b**, were determined by integrating all the emitted photons from the surface of the devices measured by a fiber optics spectrometer when a constant current was flowed on the device. All the EQE plots showed mountain shape. This is because the TTA efficiency increases with triplet concentration and become constant at high triplet concentration condition,[17] and the roll-off effect was observed at high carrier concentration. The maximum EQE values (EQE_{Max}s) of rubrene/C_{60}, rubrene/C_8-PTCDI, DBP-doped rubrene/C_{60}, and DBP-doped rubrene/C_8-PTCDI devices are 0.075%, 0.215%, 0.813%, and 2.18% respectively. The devices with C_8-PTCDI exhibited 2.9 times higher EQE than the C_{60} devices, and DBP doping increased as much as about 10 times regardless of the acceptor materials. Furthermore, the thickness of DBP doped rubrene layer was optimized and modified from the initial device with 50 nm. The device with 200 nm thick emitter layer showed highest EQE of 2.91%. This EQE value is two orders of magnitude higher than that of UC-OLED with rubrene/C_{60} bilayer in the previous report.[9] Higher EQE in the devices with thicker emitter layer suggests that escape of S_1 exciton of the emitter from the D/A is important for preventing BCS to CT state.

To clarify the energy transfer pathways from charge injection to emission in UC-OLED as illustrated in **Figure 1b**, transient EL decay was measured by a hand-made system composed of a photodiode and a transimpedance amplifier. A square voltage made by a function generator was applied to the device. In the EL decay of the rubrene/BCP control device under 6.64 V applied in **Figure 4a**, two decay components: prompt decay faster than 0.1 μs that is the detection limit of the instrument and slow decay with lifetime of 10.4 μs, were observed. Former decay is S_1 emission that is directly formed after charge injection, and the latter decay is the emission through TTA sensitized by the triplet exciton generated ether from charge injection into the rubrene or SF.[20] The amplitude of the fitted exponential revealed that 83% and 17% are from direct S1 emission and via TTA, respectively. In contrast to the rubrene/BCP control device, only one decay component with the life time of μs order was observed both in rubrene/C_8-PTCDI and DBP doped rubrene/C_8-PTCDI devices under 4.56 V applied as shown in **Figure 4b**. The results indicate that all of the EL emission from the UC-OLEDs in this study is through TTA even under higher applied voltage condition than the bandgap energy of the emitter materials. By comparing the DBP doping effect, the doping shortened the lifetime from 3.6 μs to 3.1 μs. The result indicates that EL emission could be accelerated by the DBP doping.

To evaluate the loss processes exist in the UC-OLED, obtained EQE value are compared with the ideal one. Based on the operating mechanism of UC-OLED in **Figure 1b**, the EQE of EL emission can be decomposed into efficiency of each step as follows:

$$\mathrm{EQE} = \Phi_{\mathrm{Carrier}} \times \Phi_{\mathrm{Spin}} \times \Phi_{\mathrm{TTA}} \times \Phi_{\mathrm{PL}} \times \Phi_{\mathrm{Out}} \times (1 - \Phi_{\mathrm{Loss}})$$

where Φ_{Carrier} is the carrier balance ratio of holes and electrons, Φ_{Spin} is the ratio of triplet formation, Φ_{TTA} is the TTA efficiency, Φ_{PL} is the absolute PLQE of the emitter, Φ_{Out} is the out-coupling efficiency, and Φ_{Loss} is the ratio of parasitic loss processes. Φ_{Carrier} could be regarded as 100% at the condition of $\mathrm{EQE_{Max}}$ because the EL intensity proportionally increase with carrier concentration as proved by *L-J* curves (**Figure S2**).[21] Φ_{Spin} is 75% following the spin statistics of triplet formation. Φ_{TTA} of the rubrene film has been reported to be as high as 31%,[22] when the maximum Φ_{TTA} is defined as 50%, because TTA is a two-to-one photon conversion process. Φ_{PL} was improved by DBP doping from 29.1% in the pristine rubrene to 72.6% in the 0.5% DBP-doped rubrene films, as summarized in **Table S1**,

because aggregation induced quenching and SF were suppressed. Assuming the typical Φ_{Out} value from ITO in OLED devices as 20%,[23-24] ideal EQE without parasitic loss processes in undoped and DBP doped devices are calculated to be 1.4 and 3.4%, respectively. Φ_{loss}, which is calculated by the ratio between the ideal EQE and actual values of each device, can be estimated and summarized in **Table 1**. In the case of rubrene/C_{60}, which is the combination showing smallest EQE in this study, 94% of excited states was deactivated by the loss processes. The use of C_8-PTCDI instead of C_{60} could reduce the loss processes to 84%. DBP doping further reduced, and only 14% of excited states go through the parasitic loss pathways in DBP doped rubrene/C_8-PTCDI with the optimized DBP-doped rubrene layer thickness of 200 nm. The loss processes that exist in the UC-OLEDs are illustrated in **Figure 1b**. At first, the energy of T_1 of C_{60} is about 1.6 eV that is well above that of rubrene,[25-26] thus the possibility of existence of energy transfer loss from T_1 of rubrene to C_{60} can be excluded. Suppression of SF by DBP doping is included in the improvement of Φ_{PL}. Therefore, the reduction of Φ_{Loss} by both the replacement from C_{60} to C_8-PTCDI and DBP doping is due to the suppression of either BCS from the S_1 of the emitter to the CT state and the CT state recombination at the D/A interface.

To elucidate the mechanism for the suppression of the parasitic losses at the D/A interface, CT state absorption and emission were investigated by highly sensitive incident photon to current efficiency (IPCE) and EL measurements of the devices, respectively. In IPCE spectra in **Figure 5a**, clear shoulder of photocurrent response from the CT state absorption could be observed at around 1.6 eV, which is smaller energy than the bandgap of rubrene, C_{60}, and C_8-PTCDI, both in the rubrene/C_{60} and rubrene/C_8-PTCDI devices. The CT absorption peaks can be fitted by Gaussian function.[27] The CT state energy could be calculated by the fitted curves as 1.46 and 1.40 eV in C_{60} and C_8-PTCDI devices, respectively. The strength of CT state absorption, reflecting the electronic coupling between donor and acceptor mainly dominated by the overlaps of these molecular orbitals,[27] reduced two order of magnitude from the device with C_{60} to C_8-PTCDI. The result indicates the use of C_8-PTCDI that has highly crystalline edge-on structure in the thin film greatly reduced the interaction at the D/A interface.[28] On the other hand, almost identical IPCE spectra was observed in undoped and DBP doped

devices, indicating that DBP doping did not affect the D/A interaction. The difference in the D/A interaction in CT absorption was also confirmed by the photovoltaic performance of the UC-OLED devices presented in **Figure S3**. The replacement of C_{60} to C_8-PTCDI reduced short circuit-current density (J_{SC}), which reflects charge separation probability, to less than one-third, while the DBP doping had little effect on J_{SC}. This indicates BCS loss from the S_1 of rubrene to the CT state could be reduced by the replacement of C_{60} to C_8-PTCDI. **Figure 5b** presents EL emission spectra at near-infrared region. Additional small EL emission peak could be observed in the tail of the S_1 emission in the rubrene/C_{60} devices. The peak deconvolution of the spectrum revealed the emission peak wavelength was 867 nm, which is almost same wavelength of the CT state emission of rubrene/C_{60} combination in the previous report.[11, 29] Thus, we can safely identify the emission peak at 867 nm as radiative recombination from CT to ground state, which is one of the parasitic loss in the UC-OLED. Noted that the measurement mainly detects the fluorescence from the CT_1 to ground states, but phosphorescence from CT_3 could be included. The energies of CT_1 and CT_3 are very close, calculated to be less than 10 meV,[30] thus it is very difficult to distinguish these states spectroscopically. However, the both emission are the loss processes in the UC-OLED and should be suppressed. The CT state emission disappeared by replacement of C_{60} to C_8-PTCDI. This is because C_8-PTCDI could reduce D/A interaction as revealed by highly sensitive IPCE measurement, and suppress the radiative recombination loss from the CT state. Non-radiative recombination from the CT state is also governed by the electronic coupling between the CT and the ground states that is determined by the wavefunction overlap between the donor and acceptor,[31] same as the radiative recombination, thus the reduction of D/A interfacial interaction can slow not only radiative but also non-radiative recombination rates from the CT state, resulting promotion of energy transfer from CT to T_1 of rubrene. The CT emission peak also disappeared in the DBP doped rubrene/C_{60} device. In the case of DBP doping, the D/A interaction unchanged as revealed by the IPCE measurement, thus the probability of CT state recombination should remain unchanged. Thus, the generation of the CT state by the BCS from the S_1 of the emitter should suppress by the accelerating the fluorescence by the DBP doping.

In summary, we have demonstrated efficient UC-OLED in which the bright emission over 100 cd/m^2 could be operated by only a 1.5 V battery. The EQE of the device were two order of magnitude higher than the same types of OLED in the previous report. The improvement was realized by preventing the parasitic loss processes by controlling the characteristic of the CT state: reduction of D/A interfacial interaction by the replacement of the acceptor material to the highly crystalline perylene diimide inhibited both BCS and the CT state recombination, and the addition emissive dopant kinetically suppressed BCS and SF. Our result demonstrates that the CT characteristics at the D/A interface are critically important for the management of energy transfer pathways for efficient UC, and utilizing UC emission can be one of the possible candidate for realizing efficient OLED with extremely low driving voltage.

Acknowledgements

This research was supported in part by JSPS KAKENHI, Grant-in-Aid for Young Scientists (18K14115) and Scientific Research (C) (19K04465), Mazda foundation, Kao Foundation for Arts and Sciences, and Konica Minolta Science and Technology Foundation. The authors are grateful to Mr. Tadashi Ueda, Instrument Center in Institute for Molecular Science for his assistance with PL measurements. The authors are grateful to Dr. Keisuke Tajima and Dr. Kyohei Nakano, RIKEN, for assistance with the highly sensitive IPCE measurements.

Author contributions

S.I. conceived the original idea. S.I and M.M. directed the project, designed, and performed the experiments, and wrote the paper. S.N. and M.H. supervised the research. S.I and M.M contributed equally to the work. All the authors reviewed the manuscript.

References

1. Baldo, M. A.; O'Brien, D. F.; You, Y.; Shoustikov, A.; Sibley, S.; Thompson, M. E.; Forrest, S. R., Highly efficient phosphorescent emission from organic electroluminescent devices. *Nature* **1998,** *395* (6698), 151-154.
2. Uoyama, H.; Goushi, K.; Shizu, K.; Nomura, H.; Adachi, C., Highly efficient organic light-emitting diodes from delayed fluorescence. *Nature* **2012,** *492* (7428), 234-238.
3. Su, S. J.; Sasabe, H.; Pu, Y. J.; Nakayama, K.; Kido, J., Tuning energy levels of electron-transport materials by nitrogen orientation for electrophosphorescent devices with an 'ideal' operating voltage. *Adv Mater* **2010,** *22* (30), 3311-3316.
4. Naka, S.; Okada, H.; Onnagawa, H.; Yamaguchi, Y.; Tsutsui, T., Carrier transport properties of organic materials for EL device operation. *Synth Met* **2000,** *111-112*, 331-333.
5. Tsutsui, T., Progress in Electroluminescent Devices Using Molecular Thin Films. *MRS Bull* **2013,** *22* (6), 39-45.
6. Okumoto, K.; Kanno, H.; Hamada, Y.; Takahashi, H.; Shibata, K., High efficiency red organic light-emitting devices using tetraphenyldibenzoperiflanthene-doped rubrene as an emitting layer. *Applied Physics Letters* **2006,** *89* (1), 013502.
7. Pandey, A. K.; Nunzi, J. M., Rubrene/Fullerene Heterostructures with a Half-Gap Electroluminescence Threshold and Large Photovoltage. *Adv Mater* **2007,** *19* (21), 3613-3617.
8. Xiang, C.; Peng, C.; Chen, Y.; So, F., Origin of Sub-Bandgap Electroluminescence in Organic Light-Emitting Diodes. *Small* **2015,** *11* (40), 5439-43.
9. Qiao, X.; Yuan, P.; Ma, D.; Ahamad, T.; Alshehri, S. M., Electrical pumped energy up-conversion: A non-linear electroluminescence process mediated by triplet-triplet annihilation. *Org Electron* **2017,** *46*, 1-6.
10. Yamada, M.; Naka, S.; Okada, H., Light-emitting Organic Photovoltaic Devices Based on Rubrene/PTCDI-C13 Stack. *Electrochemistry* **2017,** *85* (5), 280-282.
11. Engmann, S.; Barito, A. J.; Bittle, E. G.; Giebink, N. C.; Richter, L. J.; Gundlach, D. J., Higher order effects in organic LEDs with sub-bandgap turn-on. *Nat Commun* **2019,** *10* (1), 227.
12. Pandey, A. K., Highly efficient spin-conversion effect leading to energy up-converted electroluminescence in singlet fission photovoltaics. *Sci Rep* **2015,** *5*, 7787.
13. Chesterfield, R. J.; McKeen, J. C.; Newman, C. R.; Ewbank, P. C.; da Silva, D. A.; Bredas, J. L.; Miller, L. L.; Mann, K. R.; Frisbie, C. D., Organic thin film transistors based on N-alkyl perylene diimides: Charge transport kinetics as a function of gate voltage and temperature. *J Phys Chem B* **2004,** *108* (50), 19281-19292.
14. Izawa, S.; Shintaku, N.; Kikuchi, M.; Hiramoto, M., Importance of interfacial crystallinity to reduce open-circuit voltage loss in organic solar cells. *Appl Phys Lett* **2019,** *115* (15), 153301.
15. Huang, Z.; Simpson, D. E.; Mahboub, M.; Li, X.; Tang, M. L., Ligand enhanced upconversion of near-infrared photons with nanocrystal light absorbers. *Chem Sci* **2016,** *7* (7), 4101-4104.
16. Hiramoto, M.; Kikuchi, M.; Izawa, S., Parts-per-Million-Level Doping Effects in Organic Semiconductor Films and Organic Single Crystals. *Adv Mater* **2019,** *31* (1), e1801236.
17. Monguzzi, A.; Mezyk, J.; Scotognella, F.; Tubino, R.; Meinardi, F., Upconversion-induced fluorescence in multicomponent systems: Steady-state excitation power threshold. *Phys Rev B* **2008,** *78* (19), 195112.
18. Matsushima, T.; Bencheikh, F.; Komino, T.; Leyden, M. R.; Sandanayaka, A. S. D.; Qin, C.; Adachi, C., High performance from extraordinarily thick organic light-emitting diodes. *Nature* **2019,** *572* (7770), 502-506.
19. Park, Y.-S.; Lee, S.; Kim, K.-H.; Kim, S.-Y.; Lee, J.-H.; Kim, J.-J., Exciplex-Forming Co-host for Organic Light-Emitting Diodes with Ultimate Efficiency. *Adv Funct Mater* **2013,** *23* (39), 4914-4920.
20. Zhang, Y.; Forrest, S. R., Triplets contribute to both an increase and loss in fluorescent yield in organic light emitting diodes. *Phys Rev Lett* **2012,** *108* (26), 267404.
21. Malliaras, G. G.; Scott, J. C., The roles of injection and mobility in organic light emitting diodes. *J Appl Phys* **1998,** *83* (10), 5399-5403.
22. Di, D.; Yang, L.; Richter, J. M.; Meraldi, L.; Altamimi, R. M.; Alyamani, A. Y.; Credgington, D.; Musselman, K. P.; MacManus-Driscoll, J. L.; Friend, R. H., Efficient Triplet Exciton Fusion in Molecularly Doped Polymer Light-Emitting Diodes. *Adv Mater* **2017,** *29* (13), 1605987.

23. Smith, L. H.; Wasey, J. A. E.; Barnes, W. L., Light outcoupling efficiency of top-emitting organic light-emitting diodes. *Appl Phys Lett* **2004,** *84* (16), 2986-2988.
24. Furno, M.; Meerheim, R.; Hofmann, S.; Lüssem, B.; Leo, K., Efficiency and rate of spontaneous emission in organic electroluminescent devices. *Phys Rev B* **2012,** *85* (11), 119905.
25. Wasielewski, M. R.; O'Neil, M. P.; Lykke, K. R.; Pellin, M. J.; Gruen, D. M., Triplet states of fullerenes C_{60} and C_{70}. Electron paramagnetic resonance spectra, photophysics, and electronic structures. *J Am Chem Soc* **1991,** *113* (7), 2774-2776.
26. Arbogast, J. W.; Darmanyan, A. P.; Foote, C. S.; Diederich, F. N.; Whetten, R. L.; Rubin, Y.; Alvarez, M. M.; Anz, S. J., Photophysical properties of sixty atom carbon molecule (C_{60}). *J Phys Chem* **1991,** *95* (1), 11-12.
27. Vandewal, K.; Tvingstedt, K.; Gadisa, A.; Inganas, O.; Manca, J. V., Relating the open-circuit voltage to interface molecular properties of donor:acceptor bulk heterojunction solar cells. *Phys Rev B* **2010,** *81* (12), 125204.
28. Vandewal, K.; Widmer, J.; Heumueller, T.; Brabec, C. J.; McGehee, M. D.; Leo, K.; Riede, M.; Salleo, A., Increased open-circuit voltage of organic solar cells by reduced donor-acceptor interface area. *Adv Mater* **2014,** *26* (23), 3839-3843.
29. Ng, A. M. C.; Djurišić, A. B.; Chan, W.-K.; Nunzi, J.-M., Near infrared emission in rubrene:fullerene heterojunction devices. *Chem Phys Lett* **2009,** *474* (1), 141-145.
30. Zheng, Z.; Tummala, N. R.; Fu, Y. T.; Coropceanu, V.; Bredas, J. L., Charge-Transfer States in Organic Solar Cells: Understanding the Impact of Polarization, Delocalization, and Disorder. *ACS Appl Mater Interfaces* **2017,** *9* (21), 18095-18102.
31. Benduhn, J.; Tvingstedt, K.; Piersimoni, F.; Ullbrich, S.; Fan, Y.; Tropiano, M.; McGarry, K. A.; Zeika, O.; Riede, M. K.; Douglas, C. J.; Barlow, S.; Marder, S. R.; Neher, D.; Spoltore, D.; Vandewal, K., Intrinsic non-radiative voltage losses in fullerene-based organic solar cells. *Nat Energy* **2017,** *2* (6), 17053.

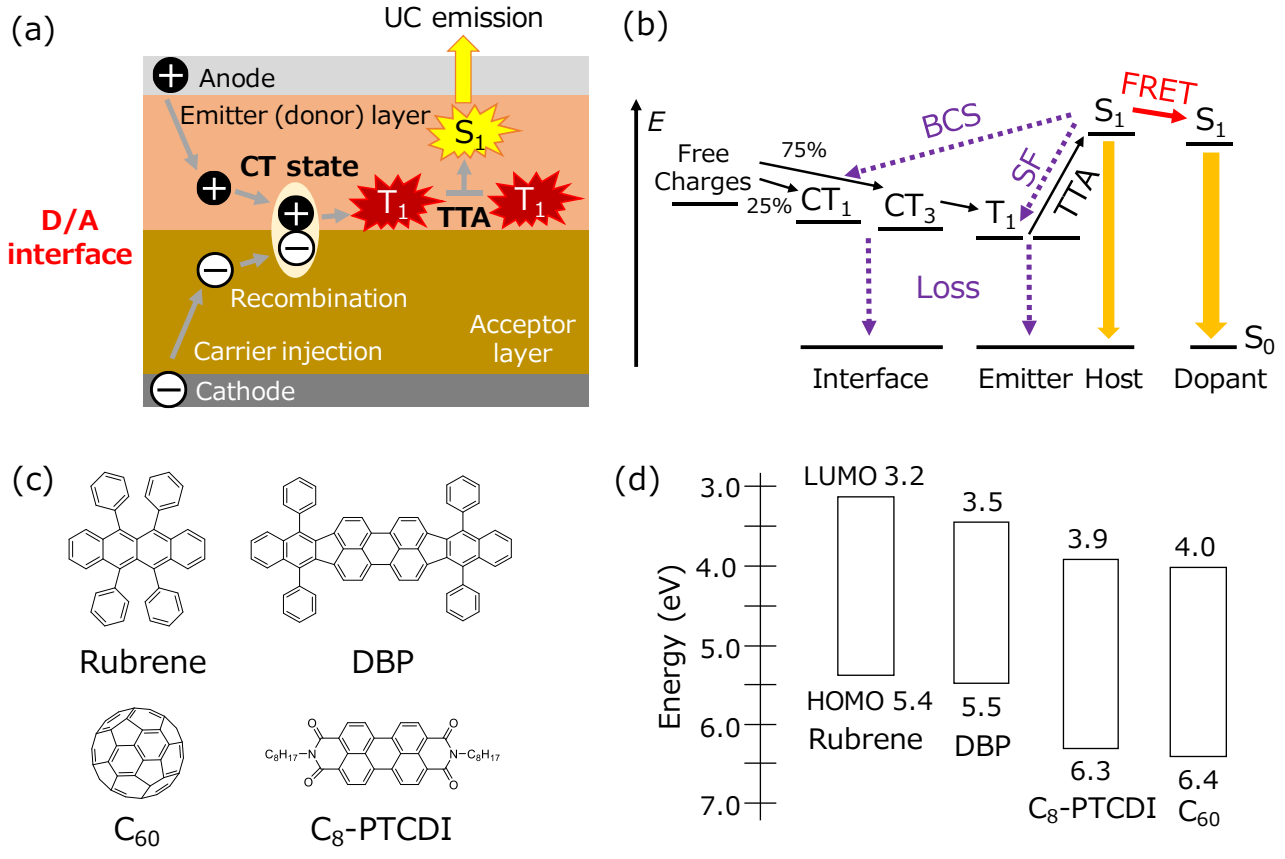

Figure 1. Schematic diagrams of (a) the device structure and (b) the state transitions in UC-OLED. (c) Chemical structures and (d) energy levels of rubrene, DBP, C_{60}, and C_8-PTCDI.

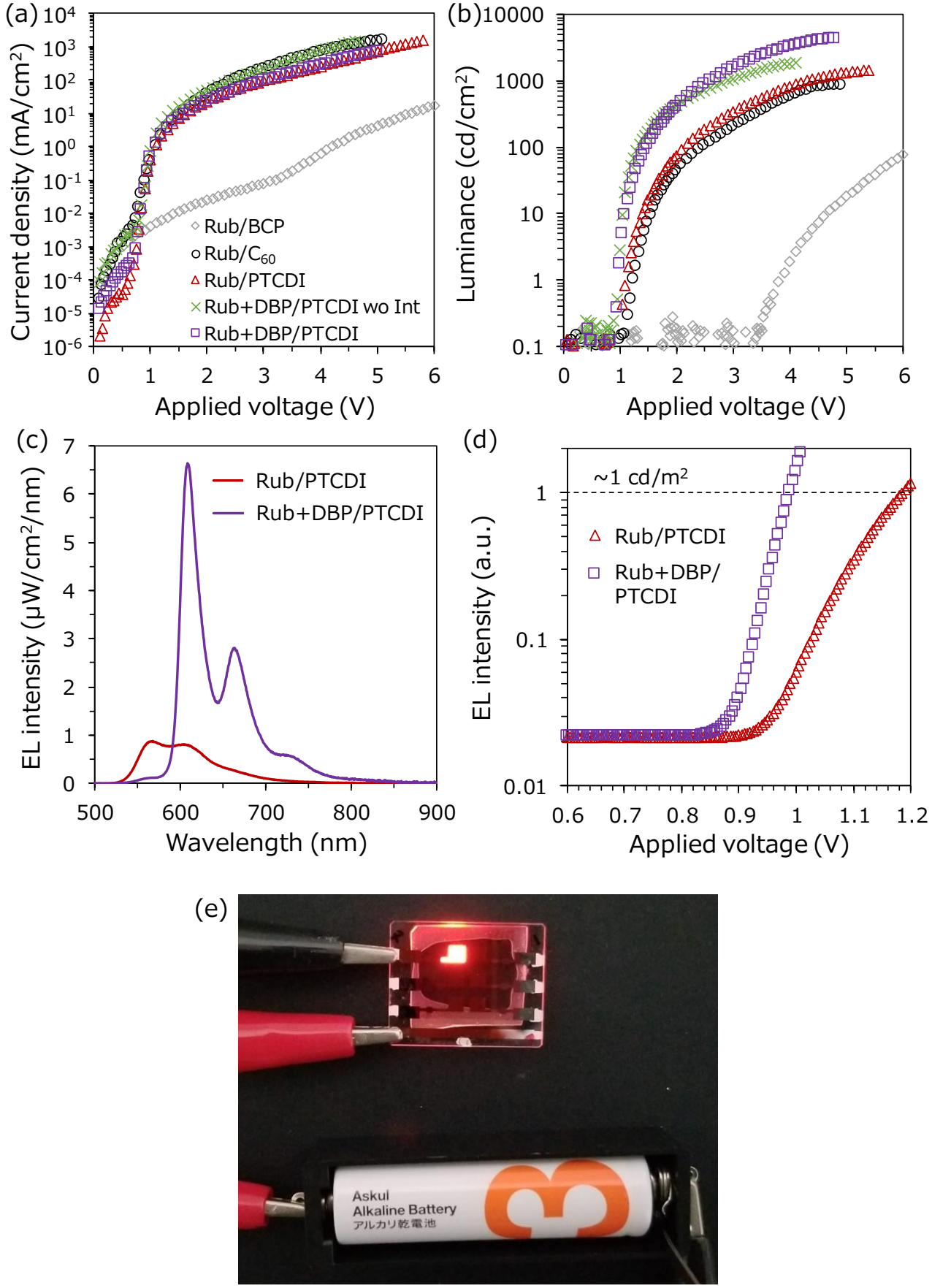

Figure 2. (a) *J-V* and (b) *L-V* curves of rubrene/BCP control (gray diamond), rubrene/C_{60} (black circle), rubrene/C_8-PTCDI (red triangle), DBP-doped rubrene/C_8-PTCDI (green cross), and DBP-doped rubrene/C_8-PTCDI (purple square) with rubrene interlayer devices. (c) EL emission spectra of

rubrene/C_8-PTCDI (red) and DBP-doped rubrene/C_8-PTCDI (purple) under constant current flow (123 mA/cm^2). (d) EL intensity as a function of applied voltage of rubrene/C_8-PTCDI (red triangle), DBP-doped rubrene/C_8-PTCDI (purple square) measured by the photodetector. The broken line indicates the condition showing EL intensity about 1 cd/m^2 measured by luminance meter. (e) Photograph of DBP-doped rubrene/C_8-PTCDI devices operated by a 1.5 V battery.

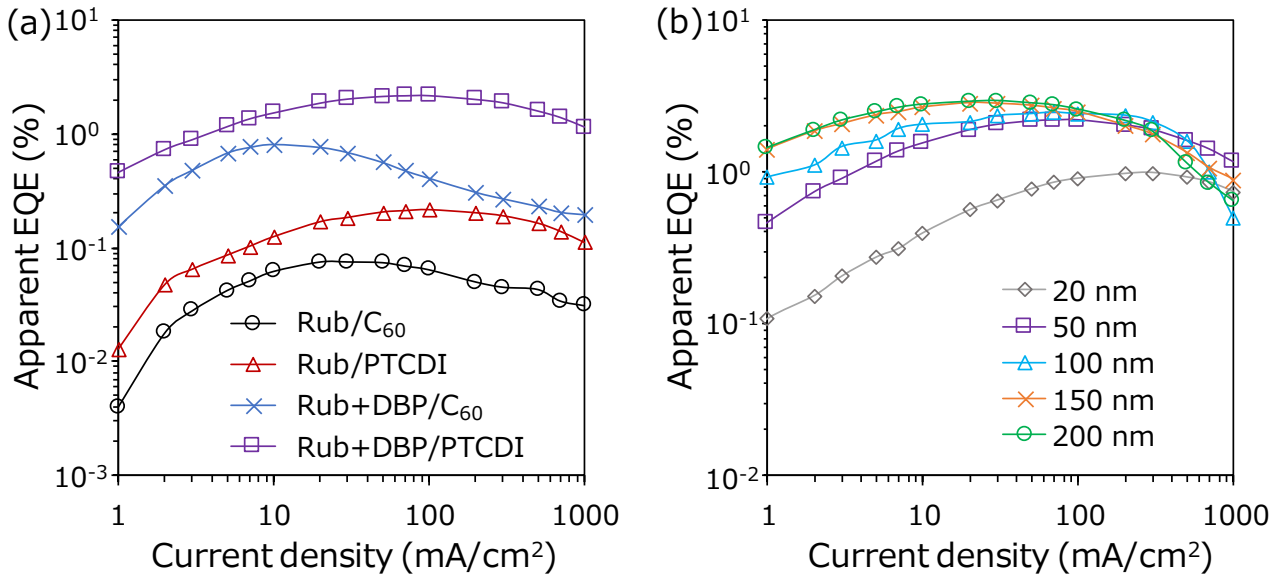

Figure 3. EQE plots as a function of injected current density (a) in rubrene/C_{60} (black circle), rubrene/C_8-PTCDI (red triangle), DBP-doped rubrene/C_{60} (blue cross), and DBP-doped rubrene/C_8-PTCDI (purple square) with the emitter layer thickness of 50 nm and (b) in the DBP-doped rubrene/C_8-PTCDI with different emitter layer thickess of 20 nm (grey diamond), 50 nm (purple square), 100 nm (blue triangle), 150 nm (orange cross), and 200 nm (green circle).

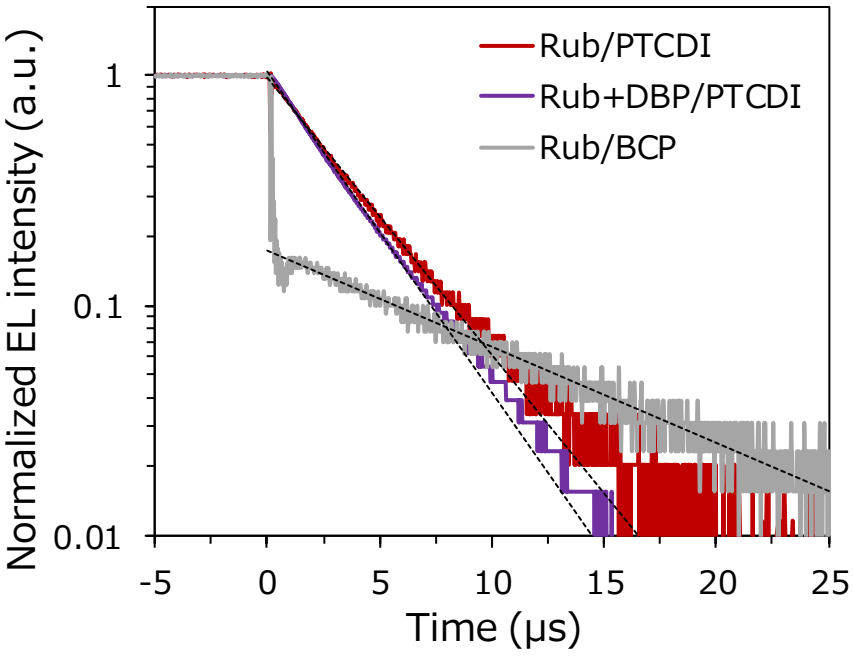

Figure 4. EL decay of (a) rubrene/BCP control (gray) and (b) rubrene/C_8-PTCDI (red) and DBP doped rubrene/C_8-PTCDI (purple) devices. The applied voltages were 6.64 V for rubrene/BCP and 4.56 V for rubrene/C_8-PTCDI and DBP doped rubrene/C_8-PTCDI devices. The EL decays were fitted by a single exponential (broken lines).

Table 1. Summary of EQE_{Max} and Φ_{Loss} values in UC-OLEDs.

	EQE_{Max}	Φ_{Loss}
Rub/C_{60}	0.075%	94%
Rub+DBP/C60	0.813%	76%
Rub/PTCDI	0.215%	84%
Rub+DBP/PTCDI 50 nm	2.18%	36%
Rub+DBP/PTCDI 100 nm	2.43%	28%
Rub+DBP/PTCDI 150 nm	2.83%	16%
Rub+DBP/PTCDI 200 nm	2.91%	14%

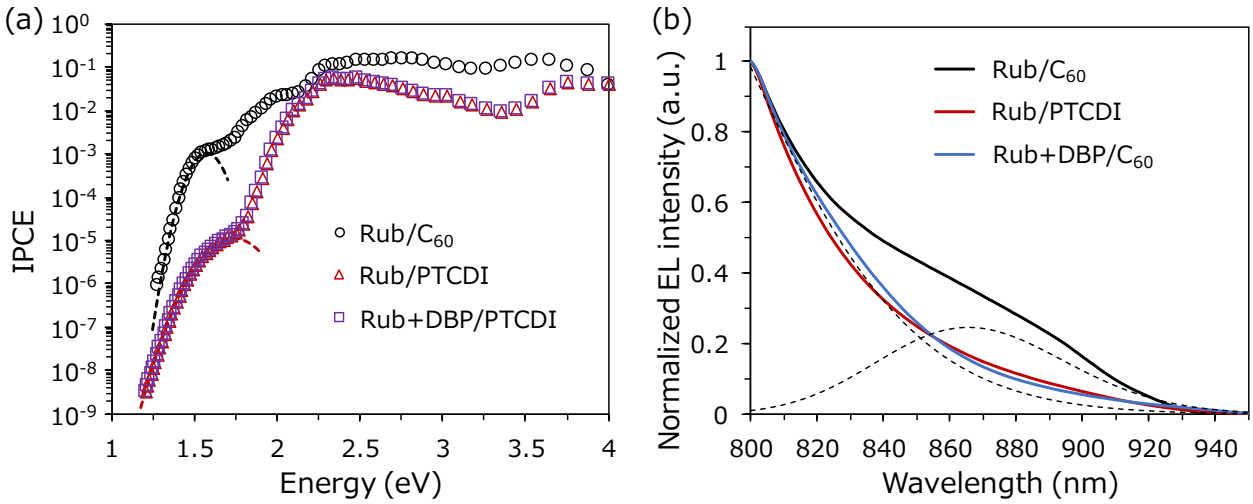

Figure 5. (a) Highly sensitive IPCE spectra of the rubrene/C_{60} (black circle), rubrene/C_8-PTCDI (red triangle), and DBP-doped rubrene/C_8-PTCDI (purple square) devices. The dashed lines represent the fitting curves of the CT state absorption by Gaussian function. (b) Normalized EL emission spectra of the rubrene/C_{60} (black), rubrene/C_8-PTCDI (red), and DBP-doped rubrene/C_{60} (blue) devices under constant current flow (308 mA/cm^2). The dashed lines represent the peak deconvolution of the EL spectrum of the rubrene/C_{60} device. The peaks were fitted by the two Gaussians as the function of photon energy.